

Review of BSM neutral Higgs results in ATLAS

Pedro Sales de Bruin* on behalf of the ATLAS collaboration[†]

University of Washington, Box 351560, Seattle WA 98195-1560, USA

E-mail: psalesde@cern.ch

The search for beyond Standard Model physics is an active area of study at the LHC. This article reviews beyond Standard Model neutral Higgs searches using Run 1 LHC proton-proton collision data with the ATLAS detector. Searches for neutral Higgs bosons decaying to $\tau\tau$ pairs, scalar particles decaying to $\gamma\gamma$ pairs, flavor-changing neutral currents involving Higgs bosons, di-Higgs decays to $b\bar{b}\gamma\gamma$ and $b\bar{b}b\bar{b}$, Higgs boson cascades and Higgs decaying to invisible particles are discussed. No significant deviations from Standard Model prediction are found, leading to tighter constraints on beyond Standard Model theories.

*Prospects for Charged Higgs Discovery at Colliders - CHARGED 2014,
16-18 September 2014
Uppsala University, Sweden*

*Speaker.

[†]Thanks to Nikolaos Rompotis, Anna Goussiou and Henry Lubatti for useful discussions.

1. Introduction

The recent discovery of a 125 GeV particle at the LHC was a great triumph of particle physics [1, 2]. This new bosonic particle is believed to be the until now unconfirmed Standard Model (SM) Higgs boson [3–8], an expectation that so far seems to be confirmed [9]. While this discovery has provided evidence for a crucial piece of the SM, there are many beyond SM theories that are also compatible with a 125 GeV scalar particle. For this reason, BSM Higgs boson searches are crucial to either confirm or exclude such scenarios and must be conducted as part of the combined effort to better understand Higgs sector physics.

The phenomenology of extended Higgs sectors can be very rich. For example, the addition of a second Higgs doublet in 2-Higgs doublet models (2HDM) leads to five Higgs bosons, two of which are charged and three are neutral with the 125 GeV Higgs being one of them [10]. The Higgs sector of the Minimal Supersymmetric Standard Model is a type-II 2HDM [11]. These extended Higgs sector models, and many others, are fully compatible with the recent 125 GeV Higgs boson discovery. In addition to introducing new particles, BSM theories can lead to enhancements or smaller values of couplings, production and decay rates with respect to Standard Model expectations [12].

This article reviews some of the searches for neutrally charged BSM Higgs bosons using 7 and 8 TeV center-of-mass energies proton proton collision data conducted by the ATLAS collaboration [13].

2. Results of ATLAS searches for neutral Beyond Standard Model Higgs bosons

2.1 $A/H/h \rightarrow \tau\tau$

A search for neutral Higgs bosons consistent with the Minimal Supersymmetric Model decaying to a $\tau\tau$ pair was conducted by ATLAS using 20.3 fb^{-1} of 8 TeV proton-proton collision data [14]. The analysis is split into three main channels depending on whether both taus decay leptonically ($\tau_{lep}\tau_{lep}$), both decay hadronically ($\tau_{had}\tau_{had}$) or one decay of each type ($\tau_{lep}\tau_{had}$). The analysis is further divided in low mass ($m_A < 200 \text{ GeV}$) and high mass ($m_A > 200 \text{ GeV}$) regimes, where m_A is the mass of the CP-odd neutral Higgs boson A . The $\tau_{lep}\tau_{lep}$ decay channel is searched only for low mass, the $\tau_{had}\tau_{had}$ only for high mass, and the $\tau_{lep}\tau_{had}$ channel is used for both. The dominant background is Z/γ^* production, which is modelled using an embedding technique consisting of replacing muons in $Z/\gamma^* \rightarrow \mu\mu$ data events with simulated τ leptons. The reconstructed τ pair invariant mass is used to look for excesses with respect to the SM prediction. Upper limits on $\tan\beta$ (the ratio of vacuum expectation values of the two Higgs doublets) as a function of the A boson mass, m_A , are set for a variety of MSSM scenarios [15], e.g. Fig. 1.

2.2 $hh \rightarrow bb\gamma\gamma$

Pair production of 125 GeV Higgs bosons can be significantly enhanced in models with extended Higgs sectors due to the possibility of a resonant decay from a heavy CP-even neutral Higgs boson [11], or even from non-resonant production which can be enhanced by models like composite Higgs [16]. ATLAS conducted a search for $hh \rightarrow b\bar{b}\gamma\gamma$ production using 20.3 fb^{-1} of 8 TeV proton-proton collision data [17]. The search includes both resonant and non-resonant di-Higgs

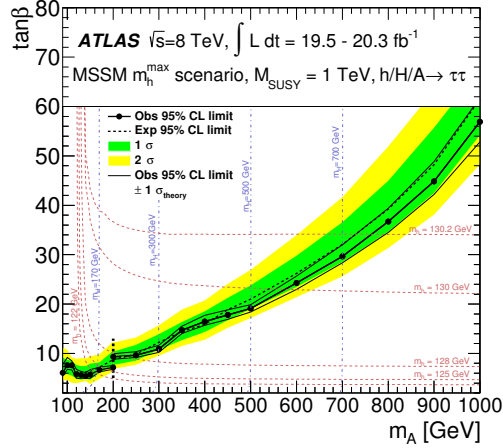


Figure 1: Upper limits on $\tan(\beta)$ as a function of m_A for the m_h^{\max} scenario of the MSSM from Ref. [14].

pair production. Upper limits on the production cross section of a narrow-width heavy scalar boson times branching ratio $\text{BR}(X \rightarrow hh)$ as a function of the heavy scalar mass are shown in Fig. 2. An upper limit on the cross section times branching ratio for the non-resonant production is set at 2.2 pb^{-1} at 95% confidence level. The observed excess has a local significance of 3.0σ . After accounting for the look-elsewhere effect, the significance is reduced to 2.1σ .

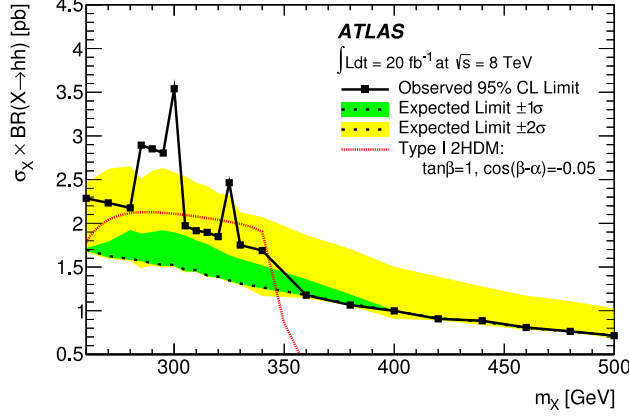


Figure 2: A 95% confidence level upper limit on the cross section times branching ratio of a narrow resonance decaying to pairs of Higgs bosons as a function of the heavy scalar mass from Ref. [17].

2.3 $hh \rightarrow bbbb$

Pair production of 125 GeV Higgs bosons from heavy resonances was also investigated in the $b\bar{b}b\bar{b}$ final state using 19.5 fb^{-1} of 8 TeV proton-proton collision data [18]. The main background process for this analysis is multi-jet production. The full selection includes the requirement of four b -tagged jets. A looser selection requiring only two b -tagged jets is used to estimate the multijet background in the signal region in a data-driven way. A distribution of the four-jet invariant mass

is shown in Fig. 3(a). The bulk Randall-Sundrum model is used as a benchmark to search for resonances, corresponding to the first Kaluza-Klein excitation mode of the graviton G^* , in the 500 to 1000 GeV mass range [19]. Observed and expected upper limits on the cross section times branching ratio as a function of the mass of the graviton, m_{G^*} , are shown in Fig. 3(b).

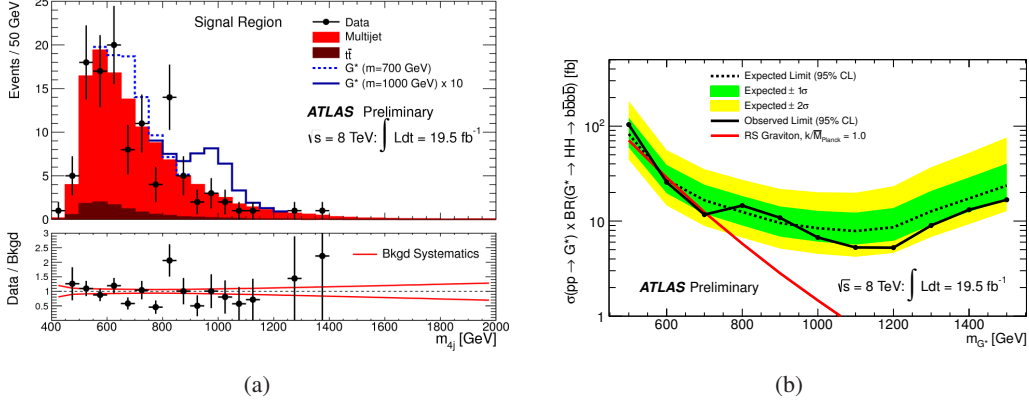


Figure 3: Comparison between predicted and observed distribution of the four-jet invariant mass after the full selection is shown in (a). Upper limits on cross section times branching ratio as a function of the mass of the graviton m_{G^*} is shown in (b). Both figures are from Ref. [18].

2.4 $X \rightarrow \gamma\gamma$

A search for neutral scalar particle in the mass range of 65 – 600 GeV that decays to a $\gamma\gamma$ pair was conducted using 20.3 fb $^{-1}$ of 8 TeV proton-proton collision data [20]. The recently discovered Higgs boson is treated as a background. The analysis is split into a low scalar mass (65 – 100 GeV) and a high scalar mass (110 – 600 GeV) regions. The main background processes are $\gamma\gamma$ and γ +jets, which are estimated using data-driven methods. The low mass analysis is further divided into three categories depending on how many photon conversions are present. Analytical functions are used for the shape of the $\gamma\gamma$ invariant mass for both signal and background. Upper limits on the fiducial cross section of a heavy scalar times branching ratio $BR(X \rightarrow \gamma\gamma)$ are set as a function of the neutral scalar mass, shown in Fig. 4.

2.5 $H \rightarrow WW$

ATLAS has also conducted a search for a high-mass Higgs boson in the $H \rightarrow WW \rightarrow l\nu l\nu$ channel using 20.7 fb $^{-1}$ of 8 TeV proton-proton collisions [21]. Due to the large Drell-Yan background in the same flavor channel, the search was restricted to cases where one W boson decayed to an electron and the other to a muon. The dominant backgrounds after the full selection come from top quark and WW production. The analysis is divided into three channels based on the jet multiplicity of the event, since this was found to significantly alter the background composition. The discriminating variable in the final likelihood fit to data is a transverse mass m_T , see Fig. 5(a). Upper limits on the cross section times branching ratio are set for both vector-boson fusion (VBF) and gluon-gluon fusion production of a SM-like scalar as a function of its mass, see Fig. 5(b).

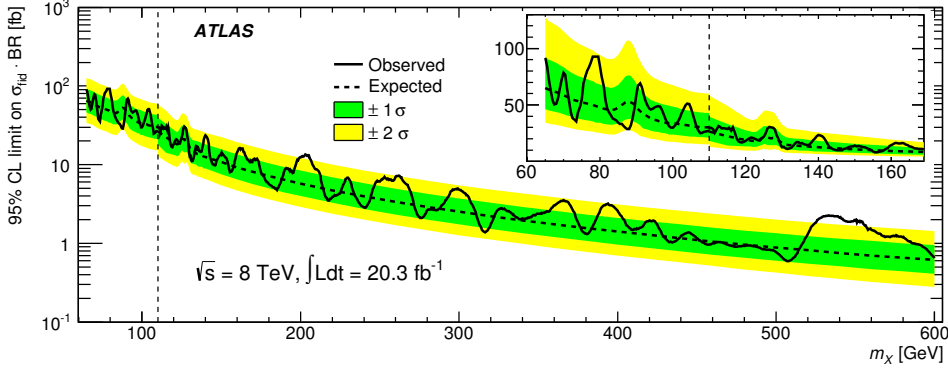


Figure 4: Observed and expected 95% confidence level limit on the fiducial cross section times branching ratio as a function of the mass of scalar mass from Ref. [20].

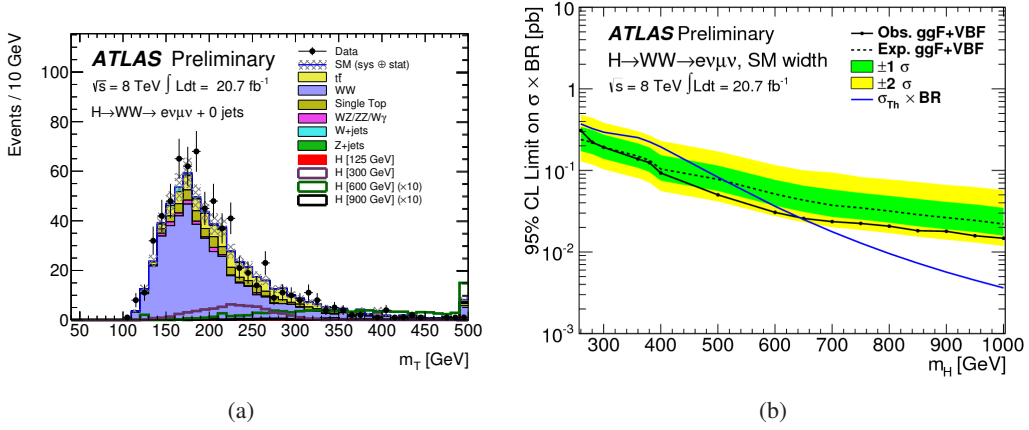


Figure 5: Transverse mass distribution for events in the 0-jet final state is shown in (a). Upper limits for a heavy scalar with a SM-like lineshape is shown in (b). Both figures are from Ref. [21].

2.6 Flavor Changing Neutral Currents using $t \rightarrow hc$

Extended Higgs sectors can sometimes present enhancements to Flavor Changing Neutral Currents (FCNC), e.g. type-III 2HDM [22]. ATLAS has looked for FCNC in $t\bar{t}$ production where one top decays to hc and the other to Wb , with $h \rightarrow \gamma\gamma$ [23]. The analysis is split into leptonic and all-hadronic search channels depending on whether the W boson decays leptonically or hadronically. The dominant background to this search is photon pair production in association with jets. The $\gamma\gamma$ invariant mass in the hadronic channel is shown in Fig. 6(a). The observed (expected) upper limit at 95% confidence level for the flavor changing branching ratio is $\text{BR}(t \rightarrow hq) < 0.79(0.51)\%$, shown in Fig. 6(b).

2.7 $H \rightarrow$ invisible

There are several BSM theories where the Higgs can couple to an invisible Dark Sector ([24]). ATLAS conducted a search for Z boson produced in association with a Higgs boson using 4.7 fb^{-1} of 7 TeV and 20.3 fb^{-1} of 8 TeV proton-proton collision data [25]. The Higgs boson is assumed

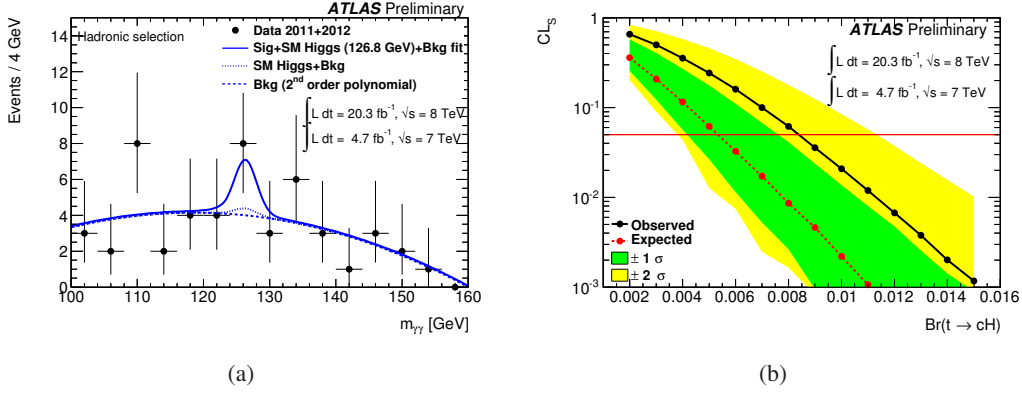


Figure 6: Distribution of the di-photon invariant mass in the all-hadronic channel is shown in (a). Evolution of the expected and observed CL_s as a function of the flavor-changing branching ratio is shown in (b), where H refers to the SM Higgs boson. Both figures are from Ref. [23].

to always decay to invisible particles, while the Z boson decays to either an electron or muon pair. The dominant background in the final event selection is from diboson production (mainly ZZ) and the missing transverse energy distribution is examined for discrepancies with respect to the SM prediction, see Fig. 7(a). Upper limits for the associated production of Higgs boson with Z boson, where the Higgs boson always decays to invisible particles, are shown in Fig. 7(b). For the 125 GeV Higgs boson an upper limit of 75% at 95% confidence level is set on the branching ratio to invisible particles.

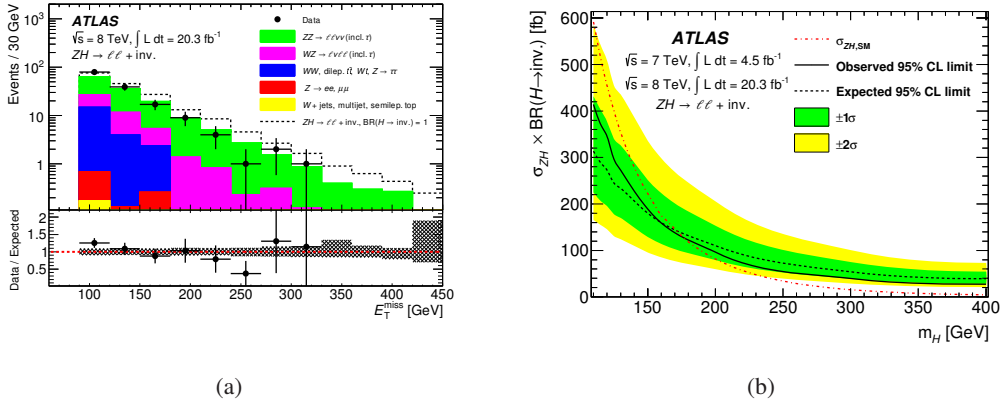


Figure 7: Distribution of the missing transverse energy after the full selection in 8 TeV data is shown in (a). Upper limits on cross section times branching ratio as a function of the Higgs boson mass is shown in (b). Both figures are from Ref. [25].

2.8 Multi-Higgs boson cascade

The presence of multiple Higgs bosons in extended Higgs sectors lead to the possibility of decay chains where a heavy Higgs can decay to a lighter Higgs. One such decay chain was searched by ATLAS using 20.3 fb^{-1} of 8 TeV proton-proton collision data [26]. This search looks for a

heavy neutral Higgs, H , produced via gluon-gluon fusion and decaying to a charged Higgs boson, H^\pm , plus a W^\mp boson. The charged Higgs boson in turn decays to a light neutral Higgs, h , and another W boson. Finally, the lightest neutral Higgs decays to $b\bar{b}$ and is assumed to have a mass of 125 GeV, see Fig. 8(a). The selection also requires one of the W bosons to decay leptonically and the other to decay hadronically. The main background after the full event selection is $t\bar{t}$, which is estimated using simulated samples. A multivariate discriminant is trained to distinguish between signal and background events using the kinematic properties of the decay objects. Upper limits on the production cross of the heavy neutral Higgs, H , times the cascade branching ratio $\text{BR}(H \rightarrow W^\pm H^\mp \rightarrow W^\pm W^\mp h \rightarrow W^\pm W^\mp b\bar{b})$ are set as a function of its mass and the charged Higgs mass and shown in Fig. 8(b).

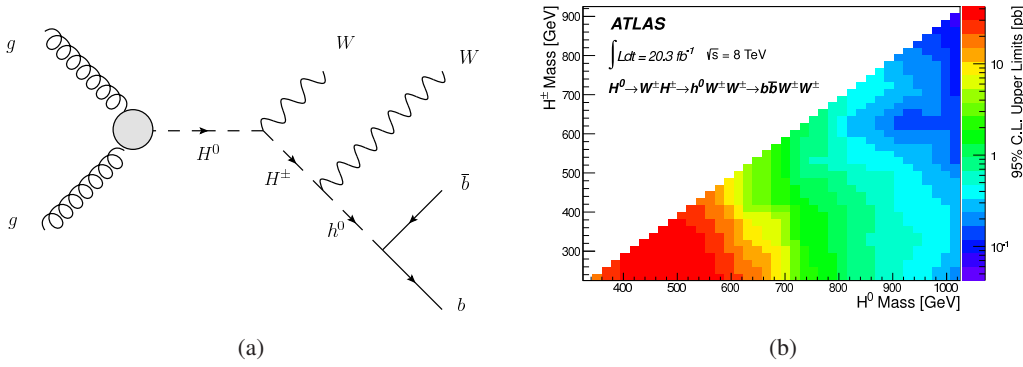


Figure 8: A diagram illustrating the Higgs boson cascade $gg \rightarrow H^0 \rightarrow WH^\pm \rightarrow WW h \rightarrow WW b\bar{b}$ is shown in (a). Observed upper limits at 95% confidence level on the cross section times branching ratio as a function of m_{H^0} and m_{H^\pm} is shown in (b). Both figures are from Ref. [26].

3. Conclusion

A number of neutral BSM Higgs searches have been conducted by the ATLAS collaboration. Recent results include tighter constraints on neutral Higgs cross sections and BSM models with neutral Higgs bosons. It is expected that the upcoming LHC run will shed additional light on whether the Higgs sector diverges from the Standard Model.

References

- [1] ATLAS Collaboration, Phys. Lett. B **716** (2012) 1 [arXiv:1207.7214 [hep-ex]].
- [2] CMS Collaboration, Phys. Lett. B **716** (2012) 30 [arXiv:1207.7235 [hep-ex]].
- [3] F. Englert and R. Brout, Phys. Rev. Lett. **13** (1964) 321.
- [4] P. W. Higgs, Phys. Lett. **12** (1964) 132.
- [5] P. W. Higgs, Phys. Rev. Lett. **13** (1964) 508.
- [6] G. S. Guralnik, C. R. Hagen and T. W. B. Kibble, Phys. Rev. Lett. **13** (1964) 585.
- [7] P. W. Higgs, Phys. Rev. **145** (1966) 1156.

- [8] T. W. B. Kibble, Phys. Rev. **155** (1967) 1554.
- [9] ATLAS Collaboration, Phys. Lett. B **726** (2013) 88 [arXiv:1307.1427 [hep-ex]].
- [10] T. D. Lee, Phys. Rev. D **8** (1973) 1226.
- [11] J. F. Gunion, H. E. Haber, G. L. Kane and S. Dawson, Front. Phys. **80** (2000) 1.
- [12] D. Curtin, R. Essig, S. Gori, P. Jaiswal, A. Katz, T. Liu, Z. Liu and D. McKeen *et al.*, Phys. Rev. D **90** (2014) 075004 [arXiv:1312.4992 [hep-ph]].
- [13] ATLAS Collaboration, JINST **3** (2008) S08003.
- [14] ATLAS Collaboration, JHEP **1411** (2014) 056 [arXiv:1409.6064 [hep-ex]].
- [15] S. Heinemeyer, W. Hollik and G. Weiglein, JHEP **0006** (2000) 009 [hep-ph/9909540].
- [16] M. Gillioz, R. Grober, C. Grojean, M. Muhlleitner and E. Salvioni, JHEP **1210** (2012) 004 [arXiv:1206.7120 [hep-ph]].
- [17] ATLAS Collaboration, arXiv:1406.5053 [hep-ex].
- [18] ATLAS collaboration, ATLAS-CONF-2014-005, <http://cds.cern.ch/record/1666518>.
- [19] H. Davoudiasl, J. L. Hewett and T. G. Rizzo, Phys. Rev. Lett. **84** (2000) 2080 [hep-ph/9909255].
- [20] ATLAS Collaboration, Phys. Rev. Lett. **113** (2014) 17, 171801 [arXiv:1407.6583 [hep-ex]].
- [21] ATLAS collaboration, ATLAS-CONF-2013-067, <http://cds.cern.ch/record/1562879>.
- [22] G. C. Branco, P. M. Ferreira, L. Lavoura, M. N. Rebelo, M. Sher and J. P. Silva, Phys. Rept. **516** (2012) 1 [arXiv:1106.0034 [hep-ph]].
- [23] ATLAS collaboration, ATLAS-CONF-2013-081, <http://cds.cern.ch/record/1565103>.
- [24] B. Patt and F. Wilczek, hep-ph/0605188.
- [25] ATLAS Collaboration, Phys. Rev. Lett. **112** (2014) 201802 [arXiv:1402.3244 [hep-ex]].
- [26] ATLAS Collaboration, Phys. Rev. D **89** (2014) 3, 032002 [arXiv:1312.1956 [hep-ex]].